

Electronic Supporting Information

**Self-Assembled Octanuclear $[Ni_5Ln_3]$ ($Ln = Dy, Tb$ and Ho) Complexes:
Synthesis, Coordination Induced Ligand Hydrolysis, Structure and
Magnetism**

Avik Bhanja,^a Eufemio Moreno-Pineda^{b,c}, Radovan Herchel^d, Wolfgang Wernsdorfer^{b,e,f},
Debashis Ray*^a

^a. Department of Chemistry, Indian Institute of Technology, Kharagpur 721302, India

^b. Institute of Nanotechnology (INT), Karlsruhe Institute of Technology (KIT), Hermann-von-Helmholtz-Platz 1,
D-76344 Eggenstein-Leopoldshafen, Germany.

^c. Depto. de Química-Física, Escuela de Química, Facultad de Ciencias Naturales, Exactas y Tecnología,
Universidad de Panamá, Panamá, Panamá.

^d. Department of Inorganic Chemistry, Faculty of Science, Palacky University, 17. listopadu 12, CZ-771 46
Olomouc, Czech Republic

^e. Physikalischs Institut, Karlsruhe Institute of Technology, D-76131 Karlsruhe, Germany.

^f. CNRS, Institut Néel, F-38042 Grenoble, France.

*Corresponding author, E-mail: dray@chem.iitkgp.ac.in

Contents

Figure S1	FTIR spectra of complex 1	3
Figure S2	Crystal packing diagram of complex 1	3
Figure S3	Observed coordination modes of ligand	4
Table S1	Results of shape measurement for Ni atoms of 1	4
Table S2	Results of shape measurement for Dy atoms of 1	4
Table S3	Crystal Data and Refinement Parameters for 1–3	5
Figure S4	Powder XRD pattern of complex 1	6
Figure S5	Powder XRD pattern of complex 2	6
Figure S6	Powder XRD pattern of complex 3	6
Figure S7	Asymmetric unit of 1	7
Figure S8	Butterfly type fused open dicubane core of 1	7
Table S4	Selected bond distances of 1	7-8
Table S5	Selected bond angles of 1	8-9
Figure S9	Molecular structure of 2	10
Table S6	Selected bond distances of 2	10-11
Table S7	Selected bond angles of 2	11-12
Figure S10	Molecular structure of 3	12
Table S8	Selected bond distances of 3	13
Table S9	Selected bond angles of 3	13-15
Figure S11	Two types of open-cubane present in complex 1	15
Figure S12	TGA graph of complex 1–3	15
Figure S13	Full range of positive mode ESI-MS spectrum of complex 1	16
Figure S14	Full range of positive mode ESI-MS spectrum of complex 2	16
Figure S15	Full range of positive mode ESI-MS spectrum of complex 3	16
Figure S16	Topological feature of complex 1	17
Figure S17	Molecular structure of previously reported Ni_5Ln_3 aggregate	17
Figure S18	CASSCF computed parameters for fragment containing Dy1	18-19
Table S10	energy barrier and principal g-tensor for fragment containing Dy1	19
Figure S19	CASSCF computed parameters for fragment containing Dy2	20
Table S11	energy barrier and principal g-tensor for fragment containing Dy2	20

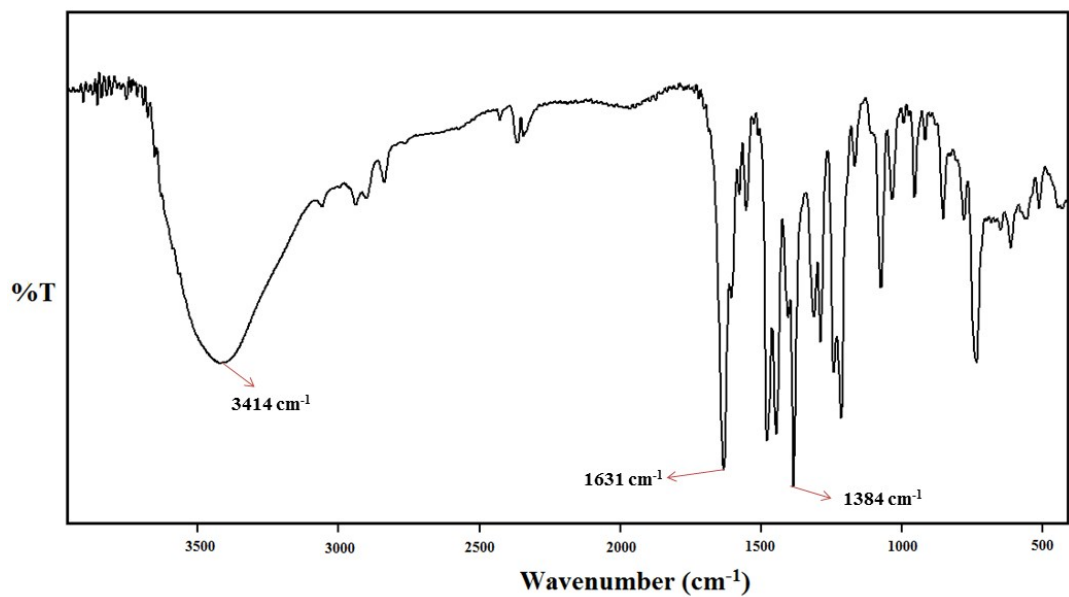


Fig. S1 FTIR spectra of complex 1

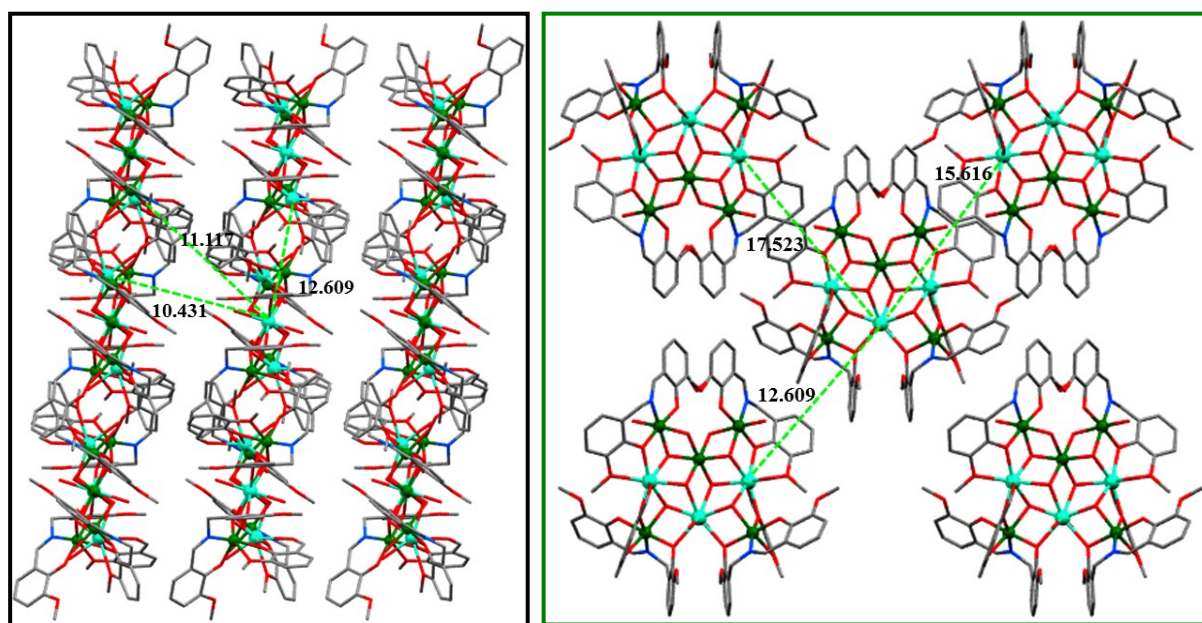


Fig. S2 (Left) Crystal packing diagram of **1** viewed along the *b* direction; (Right) Crystal packing diagram of **1** viewed along the *c* direction (counter anion, solvent molecules and H-atoms are removed for clarity)

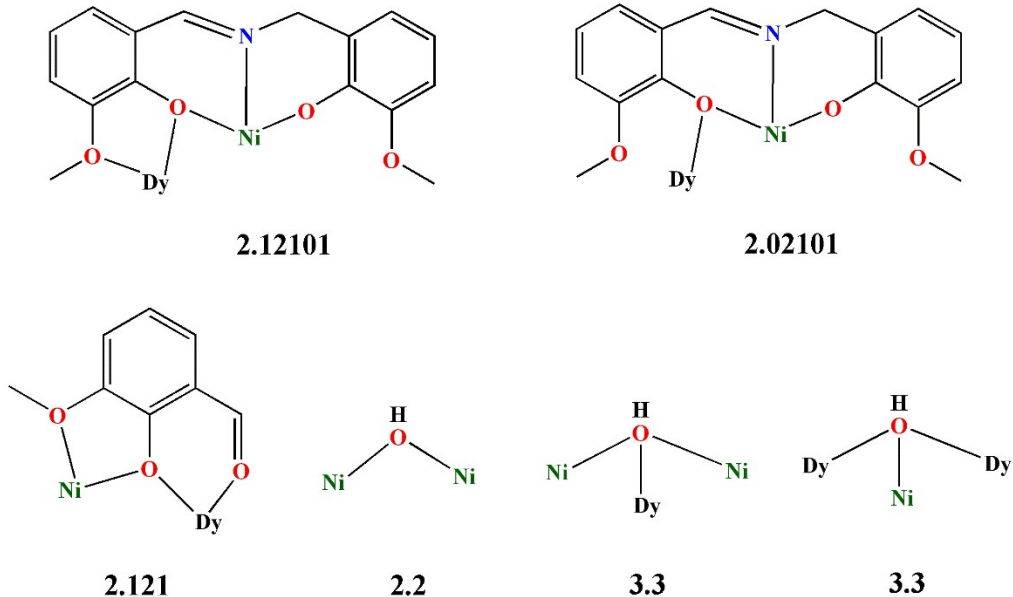


Fig. S3 Observed coordination modes^{S1} of L^{2-} , $\text{o}\text{-val}^-$ and HO^- in this work

Table S1. Results of shape measurement^{S2-S4} using program SHAPE 2.1 for Ni atoms of **1^a**

	HP-6	PPY-6	OC-6	TPR-6	JPPY-6
Ni1 of 1	31.919	23.232	1.565	12.171	27.200
Ni2 of 1	31.905	26.690	0.442	14.608	30.433
Ni3 of 1	26.593	23.838	1.123	12.060	27.203

^aHP-6 = Hexagon, PPY-6 = Pentagonal pyramid, OC-6 = Octahedron, TPR-6 = Trigonal prism, JPPY-6 = Johnson pentagonal pyramid J2

Table S2. Results of shape measurement^{S2-S4} using program SHAPE 2.1 for Dy atoms of **1^a**

	OP-8	HPY-8	HBPY-8	CU-8	SAPR-8	TDD-8	JGBF-8	JBTPR-8	BTPR-8	JSD-8	TT-8	ETBPY-8
Dy1 of 1	32.071	22.417	14.350	8.113	2.714	0.432	13.871	3.092	2.789	2.822	8.615	22.842
Dy2 of 1	32.462	22.901	15.082	8.513	0.823	2.381	14.666	3.007	2.403	4.937	9.441	24.259

^aOP-8 = Octagon, HPY-8 = Heptagonal pyramid, HBPY-8 = Hexagonal bipyramid, CU-8 = Cube, SAPR-8 = square antiprism, TDD-8 = Triangular dodecahedron, JGBF-8 = Johnson gyrobifastigium J26, JBTPR-8 = Biaugmented trigonal prism J50, BTPR-8 = Biaugmented trigonal prism, JSD-8 = Snub diphenoid J84, TT-8 = Triakis tetrahedron, ETBPY-8 = Elongated trigonal bipyramidal

Table S3. Crystal Data and Refinement Parameters for **1–3**

parameters	1	2	3
Formula	C ₈₀ H ₁₀₈ N ₅ Dy ₃ Ni ₅ O ₄₆	C ₈₀ H ₁₀₈ N ₅ Tb ₃ Ni ₅ O ₄₆	C ₈₀ H ₁₀₈ N ₅ Ho ₃ Ni ₅ O ₄₆
F.W.(g mol ⁻¹)	2656.69	2645.96	2663.98
crystal system	monoclinic	monoclinic	monoclinic
space group	C 2/c	C 2/c	C 2/c
Crystal color	Green	Green	Green
Crystal size/mm ³	0.28×0.15×0.11	0.24×0.12×0.1	0.26×0.16×0.11
limiting indices	−27 ≤ h ≤ 27 −29 ≤ k ≤ 29 −25 ≤ l ≤ 22	−21 ≤ h ≤ 26 −28 ≤ k ≤ 28 −24 ≤ l ≤ 24	−27 ≤ h ≤ 27 −29 ≤ k ≤ 29 −23 ≤ l ≤ 24
a/ Å	22.13(3)	22.194(3)	22.15(3)
b/ Å	23.55(4)	23.629(3)	23.57(4)
c/ Å	20.35(3)	20.418(3)	20.37(3)
α/ deg	90	90	90
β/ deg	96.071(17)	96.094(4)	96.081(17)
γ/ deg	90	90	90
V/ Å ³	10545(27)	10647(3)	10574(27)
D _c /g cm ⁻³	1.662	1.639	1.670
μ (mm ⁻¹)	3.061	2.918	3.175
F(000)	5396	5352	5304
θ for data collection (deg)	1.556–26.596	2.286–25.061	1.676–26.654
T/K	114(2)	114(2)	114(2)
Total reflns	67366	42298	67627
R(int)	0.0903	0.0941	0.1000
Unique reflns	10913	9397	10842
Observed reflns	7375	7615	8078
Parameters	706	707	703
R ₁ ; wR ₂ (I > 2σ(I))	0.0465, 0.1175	0.0662, 0.1970	0.0410, 0.0920
GOF (F ²)	1.036	1.042	0.986
Largest diff peak and hole (e Å ⁻³)	1.131, -1.270	3.054, -2.012	1.199, -0.885
CCDC No.	1969074	1969075	1969076

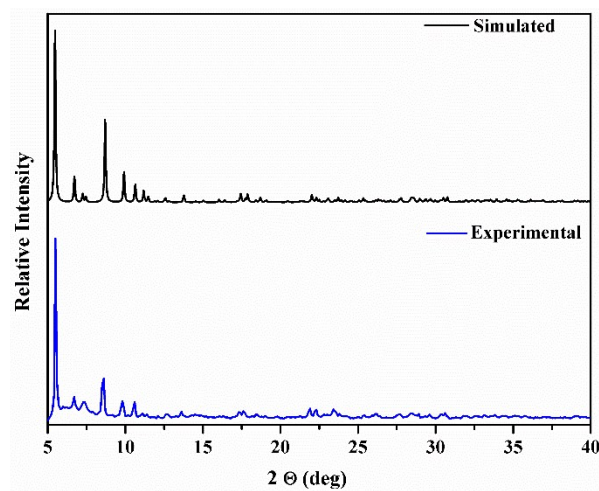


Fig. S4 Powder XRD pattern of Ni_5Dy_3 (**1**) complex

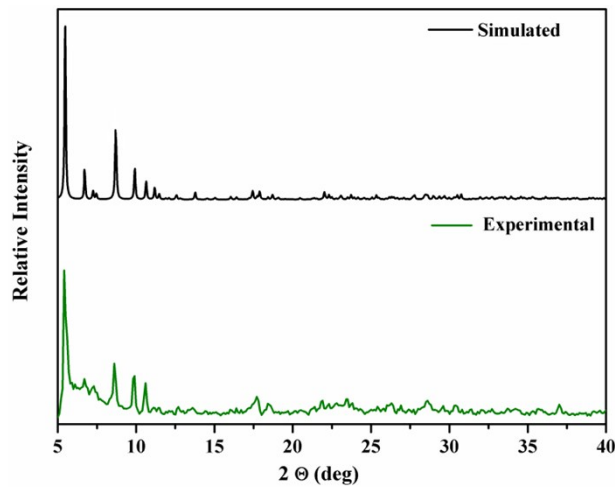


Fig. S5 Powder XRD pattern of Ni_5Tb_3 (**2**) complex

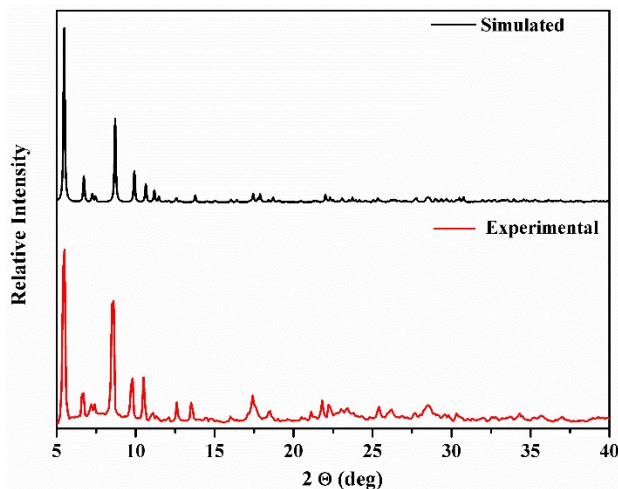


Fig. S6 Powder XRD pattern of Ni_5Ho_3 (**3**) complex

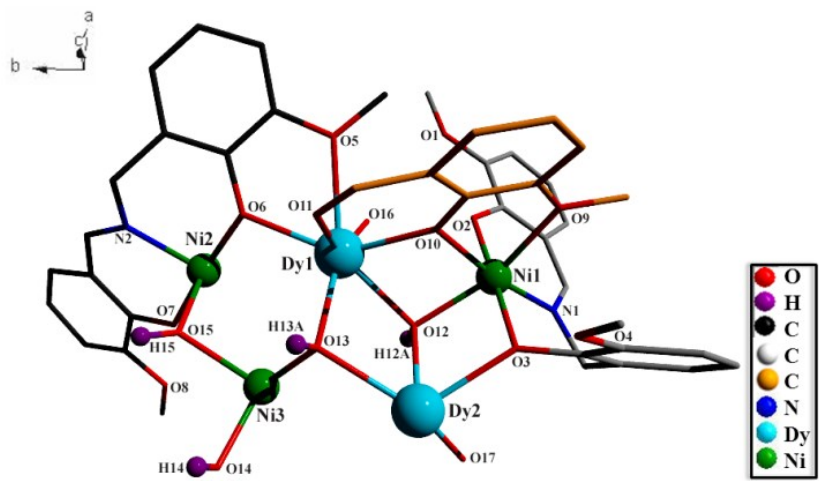


Fig. S7 Asymmetric unit of **1** with partial atom numbering scheme

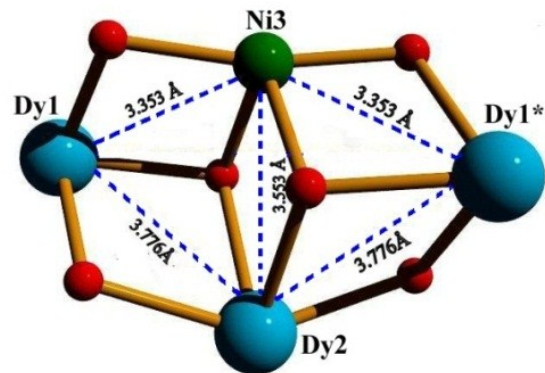


Fig. S8 Butterfly type fused open dicubane $\{ \text{NiDy}_3 \}$ central core

Table S4. Selected bond distances of **1**

Atom 1	Atom 2	Distance [Å]	Atom 1	Atom 2	Distance [Å]
Dy1	O5	2.537(5)	Ni1	O3	2.062(5)
Dy1	O6	2.264(5)	Ni1	O9	2.194(5)
Dy1	O10	2.260(5)	Ni1	O10	2.055(5)
Dy1	O11	2.432(6)	Ni1	O12	2.066(5)
Dy1	O12	2.386(5)	Ni1	N1	2.007(6)
Dy1	O13	2.313(5)	Ni2	O6	2.025(5)
Dy1	O14	2.307(5)	Ni2	O7	1.983(5)
Dy1	O16	2.379(5)	Ni2	O14	2.078(5)
Dy2	O3	2.345(5)	Ni2	O15	2.129(5)
Dy2	O3*	2.345(5)	Ni2	O18	2.083(5)
Dy2	O12	2.383(5)	Ni2	N2	1.989(6)

Dy2	O12*	2.383(5)		Ni3	O13	2.054(5)
Dy2	O13	2.417(5)		Ni3	O13*	2.054(5)
Dy2	O13*	2.417(5)		Ni3	O14	2.005(5)
Dy2	O17	2.389(5)		Ni3	O14*	2.005(5)
Dy2	O17*	2.389(5)		Ni3	O15	2.141(5)
Ni1	O2	1.989(5)		Ni3	O15*	2.141(5)

Table S5. Selected bond angles of **1**

Atom 1	Atom 2	Atom 3	Bond Angles($^{\circ}$)	Atom 1	Atom 2	Atom 3	Bond Angles($^{\circ}$)
O6	Dy1	O5	65.09(14)	O2	Ni1	O12	97.4(2)
O6	Dy1	O11	76.73(16)	O2	Ni1	N1	89.6(2)
O6	Dy1	O12	152.26(14)	O3	Ni1	O9	91.5(2)
O6	Dy1	O13	99.02(15)	O3	Ni1	O12	81.50(19)
O6	Dy1	O14	71.13(17)	O10	Ni1	O3	89.90(19)
O6	Dy1	O16	94.95(16)	O10	Ni1	O9	75.05(19)
O10	Dy1	O5	80.13(15)	O10	Ni1	O12	78.92(18)
O10	Dy1	O6	139.13(17)	O12	Ni1	O9	153.04(18)
O10	Dy1	O11	72.74(15)	N1	Ni1	O3	91.5(2)
O10	Dy1	O12	68.56(17)	N1	Ni1	O9	96.5(2)
O10	Dy1	O13	97.80(15)	N1	Ni1	O10	171.5(2)
O10	Dy1	O14	149.71(15)	N1	Ni1	O12	109.6(2)
O10	Dy1	O16	93.55(16)	O6	Ni2	O14	80.76(19)
O11	Dy1	O5	72.61(16)	O6	Ni2	O15	87.64(19)
O12	Dy1	O5	134.71(14)	O6	Ni2	O18	96.3(2)
O12	Dy1	O11	123.96(16)	O7	Ni2	O6	174.82(17)
O13	Dy1	O5	145.26(16)	O7	Ni2	O14	94.74(19)
O13	Dy1	O11	73.70(15)	O7	Ni2	O15	89.1(2)
O13	Dy1	O12	73.19(16)	O7	Ni2	O18	86.5(2)
O13	Dy1	O16	142.95(16)	O7	Ni2	N2	92.3(2)
O14	Dy1	O5	123.81(15)	O14	Ni2	O15	79.98(17)
O14	Dy1	O11	128.69(15)	O14	Ni2	O18	92.94(18)
O14	Dy1	O12	81.16(17)	O18	Ni2	O15	171.31(17)

O14	Dy1	O13	73.17(16)		N2	Ni2	O6	91.9(2)
O14	Dy1	O16	79.33(17)		N2	Ni2	O14	170.6(2)
O16	Dy1	O5	71.44(18)		N2	Ni2	O15	94.0(2)
O16	Dy1	O11	143.21(17)		N2	Ni2	O18	93.6(2)
O16	Dy1	O12	78.52(17)		O13	Ni3	O13*	83.1(3)
O3	Dy2	O3*	83.1(2)		O13	Ni3	O15	95.13(19)
O3	Dy2	O12	69.49(17)		O13	Ni3	O15*	174.21(17)
O3	Dy2	O12*	143.38(15)		O14	Ni3	O13	85.44(18)
O3	Dy2	O13	115.00(17)		O14	Ni3	O13*	103.97(18)
O3	Dy2	O13*	144.48(15)		O14	Ni3	O14*	167.6(2)
O3	Dy2	O17	86.94(16)		O14	Ni3	O15	81.33(18)
O3	Dy2	O17*	72.00(16)		O14	Ni3	O15*	89.66(18)
O12	Dy2	O12*	144.8(2)		O15	Ni3	O15*	87.2(2)
O12	Dy2	O13*	79.58(16)		Dy2	O12	Dy1	104.19(18)
O12	Dy2	O13	71.45(15)		Ni1	O12	Dy1	100.18(19)
O12	Dy2	O17	82.45(17)		Ni1	O12	Dy2	103.61(18)
O12	Dy2	O17*	106.12(17)		Dy1	O13	Dy2	105.37(16)
O13	Dy2	O13*	68.6(2)		Ni3	O13	Dy1	99.72(18)
O17	Dy2	O13*	71.73(16)		Ni3	O13	Dy2	104.1(2)
O17	Dy2	O13	135.52(14)		Ni2	O14	Dy1	102.42(19)
O17	Dy2	O17*	152.0(2)		Ni3	O14	Dy1	101.42(18)
O2	Ni1	O3	178.66(17)		Ni3	O14	Ni2	100.82(18)
O2	Ni1	O9	89.2(2)		Ni2	O15	Ni3	94.93(19)
O2	Ni1	O10	89.2(2)		Ni1	O10	Dy1	104.82(19)

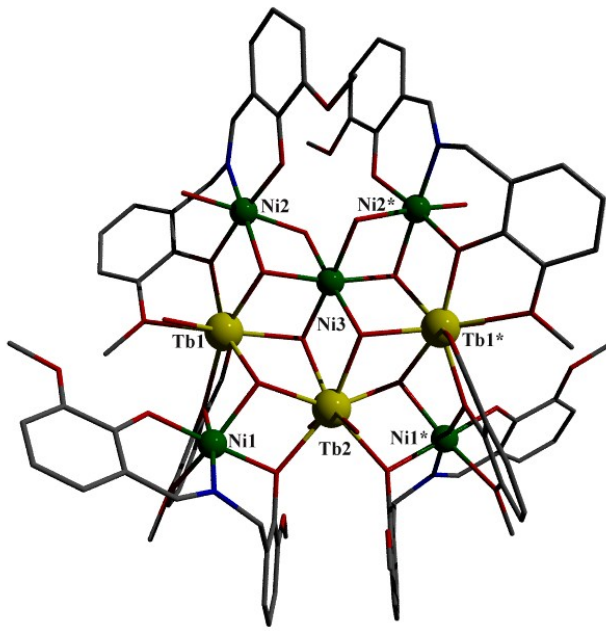


Fig. S9 Molecular structure of complex **2**. H atoms are omitted for clarity. Colour code: C, grey; O, red; N, blue.

Table S6. Selected bond distances of **2**

Atom 1	Atom 2	Distance [Å]	Atom 1	Atom 2	Distance [Å]
Tb1	O5	2.565(6)	Ni1	O3	2.075(6)
Tb1	O6	2.270(5)	Ni1	O9	2.191(6)
Tb1	O10	2.283(6)	Ni1	O10	2.049(6)
Tb1	O11	2.450(6)	Ni1	O12	2.086(6)
Tb1	O12	2.402(5)	Ni1	N1	2.009(7)
Tb1	O13	2.325(5)	Ni2	O6	2.037(6)
Tb1	O14	2.327(6)	Ni2	O7	1.976(6)
Tb1	O16	2.400(6)	Ni2	O14	2.075(5)
Tb2	O3	2.363(6)	Ni2	O15	2.135(6)
Tb2	O3	2.363(6)	Ni2	O18	2.084(6)
Tb2	O12	2.403(5)	Ni2	N2	2.000(8)
Tb2	O12*	2.403(5)	Ni3	O13	2.047(5)
Tb2	O13	2.440(5)	Ni3	O13*	2.047(6)
Tb2	O13*	2.440(5)	Ni3	O14	2.014(5)
Tb2	O17	2.407(5)	Ni3	O14*	2.014(5)
Tb2	O17*	2.407(5)	Ni3	O15	2.156(6)
Ni1	O2	1.992(6)	Ni3	O15*	2.156(6)

Table S7. Selected bond angles of **2**

Atom 1	Atom 2	Atom 3	Bond Angles($^{\circ}$)	Atom 1	Atom 2	Atom 3	Bond Angles($^{\circ}$)
O6	Tb1	O5	64.85(19)	O2	Ni1	O12	97.2(2)
O6	Tb1	O10	139.3(2)	O2	Ni1	N1	89.8(3)
O6	Tb1	O11	77.4(2)	O3	Ni1	O9	91.0(2)
O6	Tb1	O12	152.18(19)	O3	Ni1	O12	82.0(2)
O6	Tb1	O13	99.17(19)	O10	Ni1	O3	89.9(2)
O6	Tb1	O14	70.87(18)	O10	Ni1	O9	75.0(2)
O6	Tb1	O16	94.0(2)	O10	Ni1	O12	79.3(2)
O10	Tb1	O5	80.5(2)	O12	Ni1	O9	153.4(2)
O10	Tb1	O11	72.2(2)	N1	Ni1	O3	91.0(3)
O10	Tb1	O12	68.49(19)	N1	Ni1	O9	96.0(3)
O10	Tb1	O13	97.44(19)	N1	Ni1	O10	171.0(3)
O10	Tb1	O14	149.84(19)	N1	Ni1	O12	109.7(3)
O10	Tb1	O16	94.7(2)	O6	Ni2	O14	80.8(2)
O11	Tb1	O5	72.86(19)	O6	Ni2	O15	88.1(2)
O12	Tb1	O5	134.88(19)	O6	Ni2	O18	95.5(3)
O12	Tb1	O11	123.48(19)	O7	Ni2	O6	174.8(2)
O13	Tb1	O5	145.14(19)	O7	Ni2	O14	94.7(2)
O13	Tb1	O11	73.44(19)	O7	Ni2	O15	88.6(2)
O13	Tb1	O12	73.22(18)	O7	Ni2	O18	87.3(3)
O13	Tb1	O14	72.79(19)	O7	Ni2	N2	92.3(3)
O13	Tb1	O16	142.97(19)	O14	Ni2	O18	92.8(2)
O14	Tb1	O5	123.86(19)	O18	Ni2	O15	171.8(2)
O14	Tb1	O11	128.38(19)	N2	Ni2	O6	91.8(3)
O14	Tb1	O12	81.35(18)	N2	Ni2	O14	170.5(3)
O14	Tb1	O16	79.2(2)	N2	Ni2	O15	93.3(3)
O16	Tb1	O5	71.4(2)	N2	Ni2	O18	93.9(3)
O16	Tb1	O11	143.5(2)	O13	Ni3	O13*	82.7(3)
O16	Tb1	O12	79.07(19)	O13	Ni3	O15	95.4(2)
O3	Tb2	O3*	82.9(3)	O13	Ni3	O15*	174.0(2)

O3	Tb2	O12	69.89(19)		O14	Ni3	O13*	104.2(2)
O3	Tb2	O12*	143.43(19)		O14	Ni3	O13	85.6(2)
O3	Tb2	O13*	144.80(19)		O14	Ni3	O14*	167.1(3)
O3	Tb2	O13	115.52(18)		O14	Ni3	O15	81.3(2)
O3	Tb2	O17	71.9(2)		O14	Ni3	O15*	89.3(2)
O3	Tb2	O17*	86.8(2)		O15	Ni3	O15*	87.1(3)
O12	Tb2	O12*	144.3(3)		Ni1	O3	Tb2	104.6(2)
O12	Tb2	O13	71.21(18)		Ni1	O10	Tb1	104.7(2)
O12	Tb2	O13*	79.18(18)		Ni1	O12	Tb1	99.6(2)
O12	Tb2	O17*	106.39(18)		Ni1	O12	Tb2	102.9(2)
O12	Tb2	O17	82.37(18)		Tb1	O13	Tb2	105.3(2)
O13	Tb2	O13*	67.3(3)		Ni3	O13	Tb1	100.2(2)
O17	Tb2	O13	134.99(19)		Ni3	O13	Tb2	105.0(2)
O17	Tb2	O13*	72.48(19)		Ni2	O14	Tb1	102.5(2)
O17	Tb2	O17*	151.8(3)		Ni3	O14	Tb1	101.1(2)
O2	Ni1	O3	179.0(2)		Ni3	O14	Ni2	100.9(2)
O2	Ni1	O9	89.6(3)		Ni2	O15	Ni3	94.5(2)
O2	Ni1	O10	89.5(2)		Tb1	O12	Tb2	104.0(2)

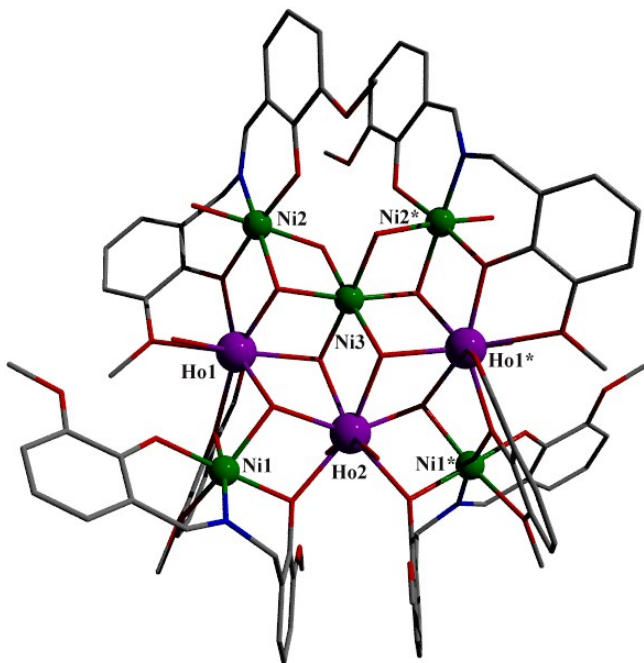


Fig. S10 Molecular structure of complex 3. H atoms are omitted for clarity. Colour code: C, grey; O, red; N, blue.

Table S8. Selected bond distances of **3**

Atom 1	Atom 2	Distance [Å]	Atom 1	Atom 2	Distance [Å]
Ho1	O5	2.529(5)	Ni1	O3	2.053(4)
Ho1	O6	2.259(4)	Ni1	O9	2.184(4)
Ho1	O10	2.263(5)	Ni1	O10	2.048(4)
Ho1	O11	2.409(5)	Ni1	O12	2.067(4)
Ho1	O12	2.373(4)	Ni1	N1	2.005(5)
Ho1	O13	2.287(5)	Ni2	O6	2.035(4)
Ho1	O14	2.307(4)	Ni2	O7	1.978(4)
Ho1	O16	2.358(4)	Ni2	O14	2.078(4)
Ho2	O3	2.349(4)	Ni2	O15	2.123(4)
Ho2	O3*	2.349(4)	Ni2	O18	2.067(4)
Ho2	O12	2.364(4)	Ni2	N2	2.002(5)
Ho2	O12*	2.364(4)	Ni3	O13	2.062(4)
Ho2	O13	2.407(4)	Ni3	O13*	2.062(4)
Ho2	O13*	2.408(4)	Ni3	O14	1.990(4)
Ho2	O17	2.365(5)	Ni3	O14*	1.990(4)
Ho2	O17*	2.365(5)	Ni3	O15	2.144(4)
Ni1	O2	1.980(4)	Ni3	O15*	2.144(4)

Table S9. Selected bond angles of **3**

Atom 1	Atom 2	Atom 3	Bond Angles(°)	Atom 1	Atom 2	Atom 3	Bond Angles(°)
O6	Ho1	O5	65.18(12)	O2	Ni1	O12	96.99(18)
O6	Ho1	O10	139.01(14)	O3	Ni1	O9	90.92(18)
O6	Ho1	O11	76.66(14)	O3	Ni1	O12	81.88(17)
O6	Ho1	O12	152.88(12)	O10	Ni1	O3	90.17(16)
O6	Ho1	O13	99.54(13)	O10	Ni1	O9	75.46(17)
O6	Ho1	O14	70.82(15)	O10	Ni1	O12	78.22(15)
O6	Ho1	O16	94.50(14)	O12	Ni1	O9	152.67(15)
O10	Ho1	O5	79.59(12)	N1	Ni1	O3	91.11(18)
O10	Ho1	O11	73.05(12)	N1	Ni1	O9	95.98(19)
O10	Ho1	O12	68.05(14)	N1	Ni1	O10	171.37(16)

O10	Ho1	O13	97.70(13)		N1	Ni1	O12	110.42(18)
O10	Ho1	O14	150.12(12)		O6	Ni2	O14	80.07(17)
O10	Ho1	O16	93.50(13)		O6	Ni2	O15	87.59(16)
O11	Ho1	O5	72.31(13)		O6	Ni2	O18	96.79(18)
O12	Ho1	O5	134.35(12)		O7	Ni2	O6	174.62(14)
O12	Ho1	O11	123.60(14)		O7	Ni2	O14	95.41(17)
O13	Ho1	O5	145.04(14)		O7	Ni2	O15	88.76(18)
O13	Ho1	O11	73.59(13)		O7	Ni2	O18	86.29(18)
O13	Ho1	O12	73.00(14)		O14	Ni2	O15	79.88(15)
O13	Ho1	O14	73.44(14)		O18	Ni2	O14	92.98(15)
O13	Ho1	O16	143.13(13)		O18	Ni2	O15	170.90(14)
O14	Ho1	O5	124.03(13)		N2	Ni2	O6	91.87(19)
O14	Ho1	O11	128.22(13)		N2	Ni2	O14	169.75(16)
O14	Ho1	O12	82.09(16)		N2	Ni2	O15	93.57(18)
O14	Ho1	O16	79.43(15)		N2	Ni2	O18	94.25(18)
O16	Ho1	O5	71.56(16)		O13	Ni3	O13*	81.6(2)
O16	Ho1	O11	143.16(14)		O13	Ni3	O15*	173.53(14)
O16	Ho1	O12	79.00(15)		O13	Ni3	O15	95.83(17)
O3	Ho2	O3*	82.2(2)		O14	Ni3	O13*	104.22(15)
O3	Ho2	O12	69.92(15)		O14	Ni3	O13	85.34(15)
O3	Ho2	O12*	143.48(13)		O14	Ni3	O14*	167.54(19)
O3	Ho2	O13	115.69(15)		O14	Ni3	O15*	89.60(15)
O3	Ho2	O13*	144.67(13)		O14	Ni3	O15	81.37(15)
O3	Ho2	O17*	86.31(13)		O15	Ni3	O15*	87.4(2)
O3	Ho2	O17	71.99(13)		Ni1	O3	Ho2	104.39(17)
O12	Ho2	O12*	144.43(18)		Ni2	O6	Ho1	106.10(17)
O12	Ho2	O13	71.06(14)		Ni1	O10	Ho1	105.29(16)
O12	Ho2	O13*	79.53(14)		Ho2	O12	Ho1	104.36(16)
O12	Ho2	O17*	106.01(15)		Ni1	O12	Ho1	100.88(17)
O12	Ho2	O17	82.86(15)		Ni1	O12	Ho2	103.41(16)
O13	Ho2	O13*	68.02(19)		Ho1	O13	Ho2	105.69(14)

O17	Ho2	O13	135.56(12)		Ni3	O13	Ho1	99.71(15)
O17	Ho2	O13*	72.36(14)		Ni3	O13	Ho2	105.21(18)
O17	Ho2	O17*	151.30(18)		Ni2	O14	Ho1	102.97(17)
O2	Ni1	O3	178.85(14)		Ni3	O14	Ho1	101.24(16)
O2	Ni1	O9	90.00(19)		Ni3	O14	Ni2	101.04(15)
O2	Ni1	O10	89.38(17)		Ni2	O15	Ni3	94.78(16)

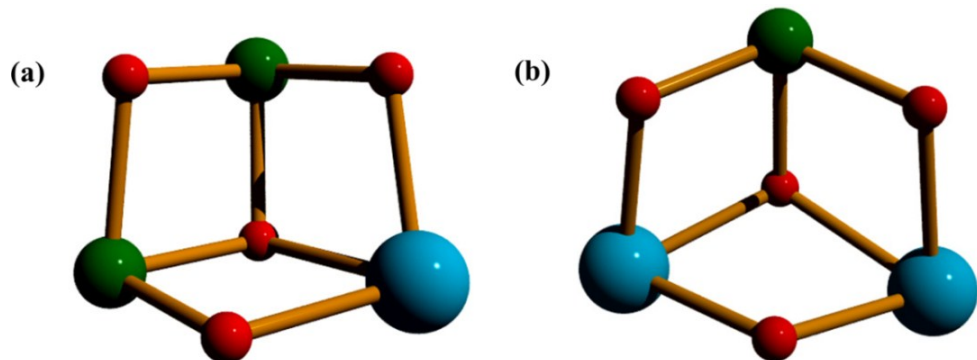


Fig. S11 Two types of open-cubane present in the structure (a) Ni_2DyO_3 and (b) Dy_2NiO_3

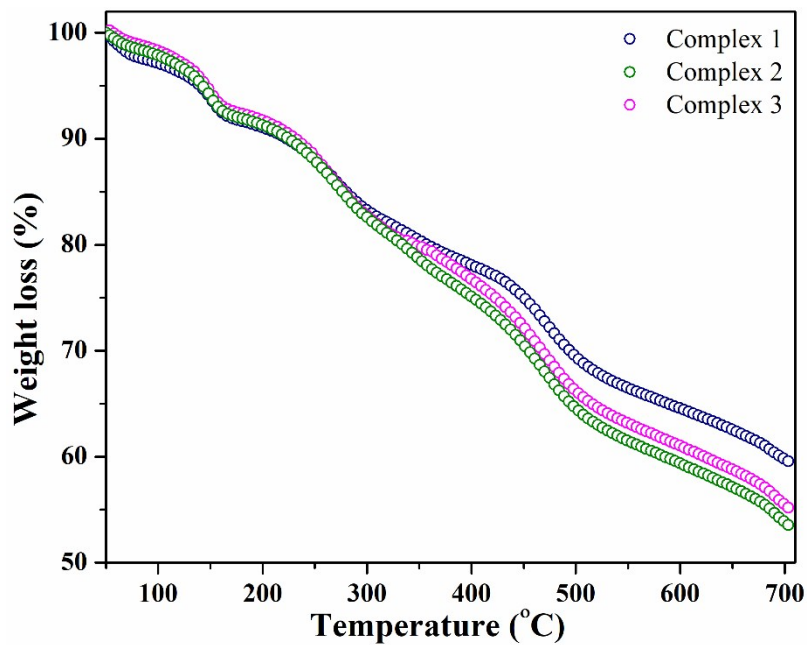


Fig. S12 TGA curves of complexes **1-3**. The % of weight loss in the temperature range 50–125 °C is: **1**; 4.54, **2**; 4.67, **3**; 4.49.

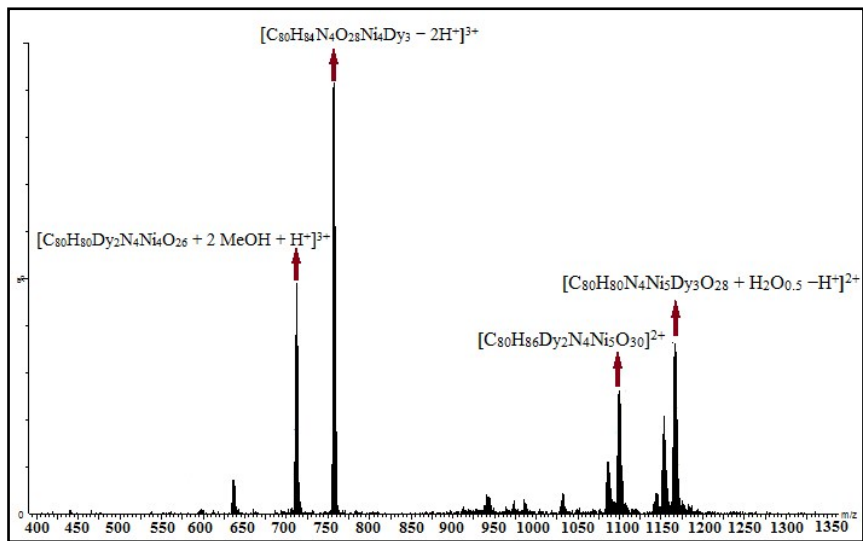


Fig. S13 Full range of positive mode ESI-MS spectrum of complex 1.

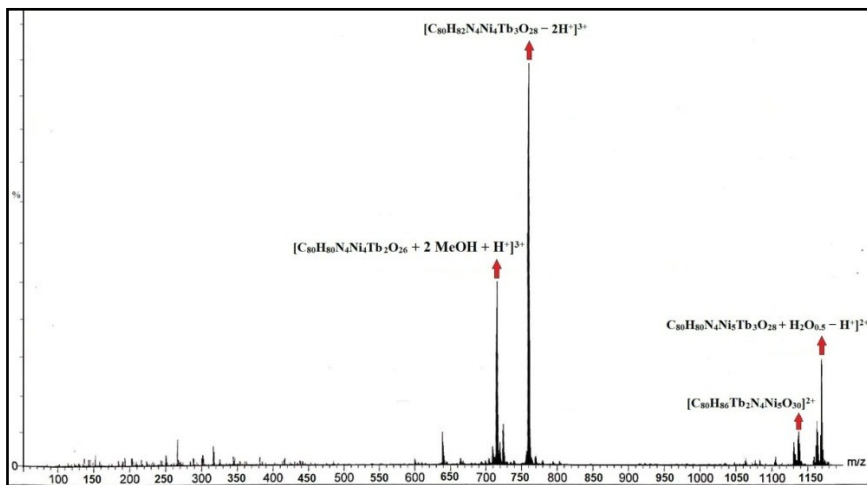


Fig. S14 Full range of positive mode ESI-MS spectrum of complex 2.

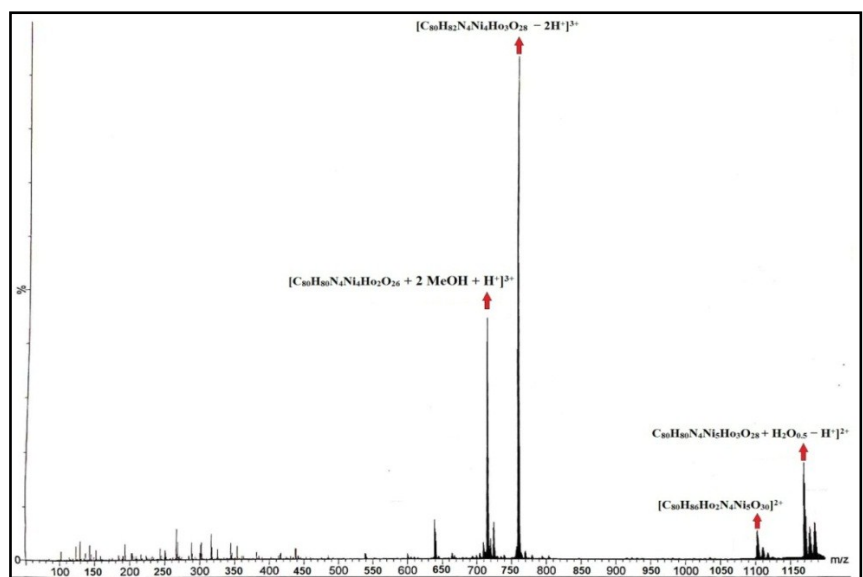


Fig. S15 Full range of positive mode ESI-MS spectrum of complex 3.

Topological Description. Topological description of the key structural features of complexes **1**, **2** and **3** was carried out using methods for the topological analysis as established by Kostakis *et al.*^{S5–S7} The analysis revealed that the Ni₅Ln₃ cluster can be described by the symbol 2,4,5M8–2. The 2,4,5M8–2 motif is comprised of six fused triangles; where four of them consist of two Ln^{III} and one Ni^{II} node and two of them has two Ni^{II} and one Ln^{III} node (Figure 8). The survey of the database^{S8} revealed that there are few reports of homometallic octanuclear clusters such as Fe₈^{S9–S10}, Co₈^{S11}, Ni₈^{S12} having the same motif. Thus, according to our knowledge this is the first example of the 2,4,5M8–2 motif in heteronuclear cluster family incorporating both 3d and 4f ions in two different coordination geometry.

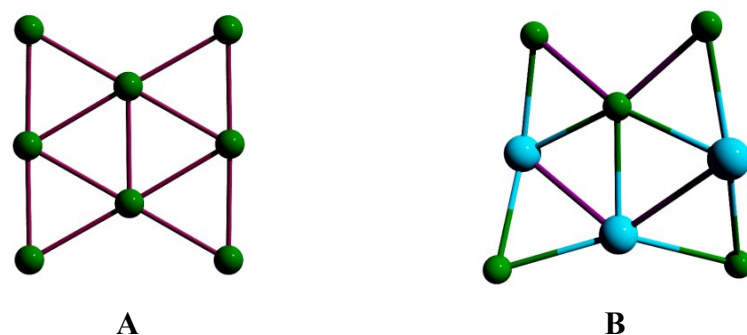


Fig. S16 **A:** 2,4,5M8–2 topological network for the reported Ni₈ cluster^{S12}; **B:** 2,4,5M8–2 topology for the present work. Green and light blue nodes represent the Ni^{II} and Ln^{III} ions.

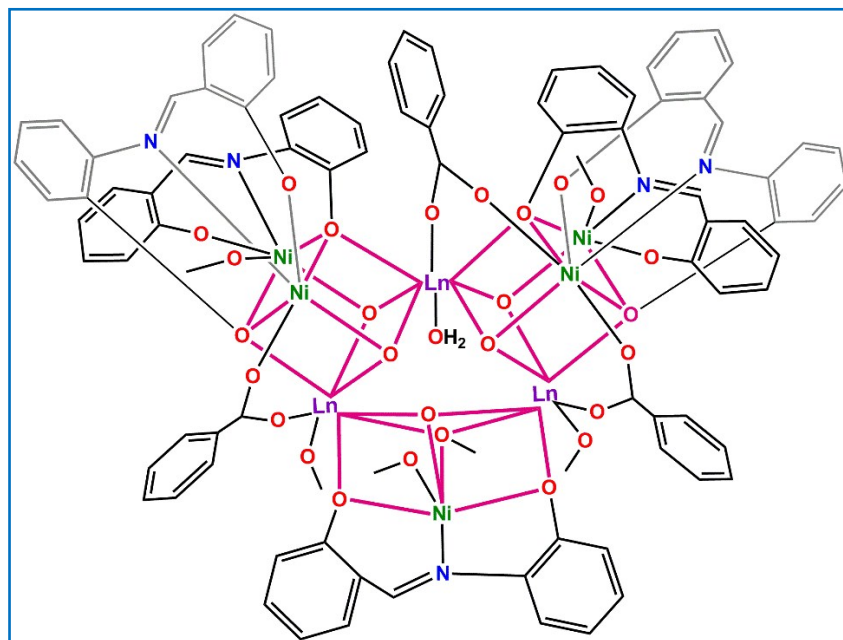
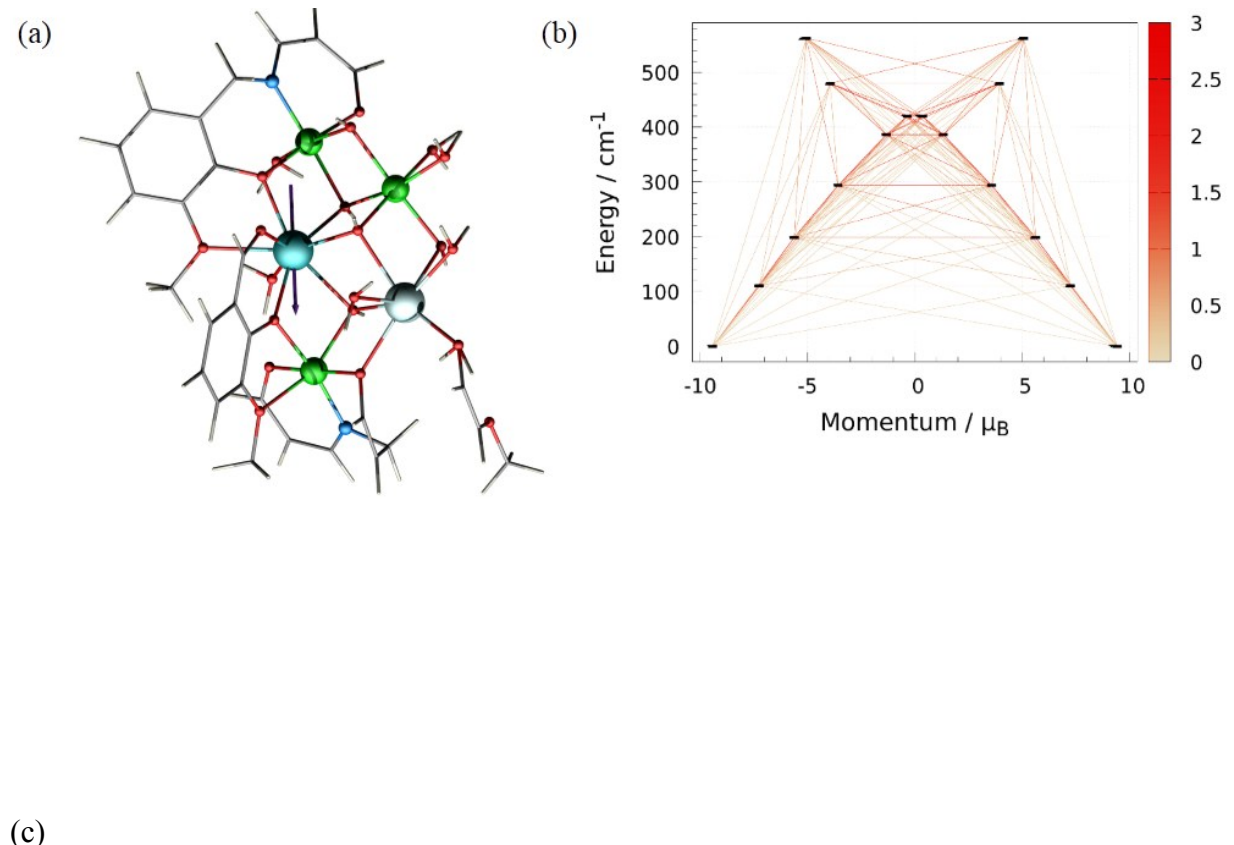


Fig. S17 Molecular structure of previously reported Ni₅Ln₃ aggregate

CASSCF Calculation: *ab initio* calculations were performed with the CASSCF/SO-RASSI/SINGLE_ANISO approach implemented in the OpenMOLCAS 19.11 program package. For this, the crystal structure of Ni_5Dy_3 was employed without further optimisation, with the atoms being described using standard basis sets from the ANO-RCC library available in Molcas. Due to the large size of the complex, and the computational cost, the molecule was split in two pentanuclear fragments as shown in figure S18 and S19. For the dysprosium ion a basis set of VQZP quality employed, whilst VDZP quality was used for the oxygen atoms directly attached to the lanthanide ions, and MB quality for all remaining atoms. The molecular orbitals (MOs) were optimized in state-averaged CASSCF calculations. For this, the active space was defined by the nine 4f electrons in the seven 4f orbitals of Dy(III). Three calculations were performed independently for each possible spin state, where 21 roots were included for $S = 5/2$, 224 roots were included for $S = 3/2$, and 490 roots were for $S = 1/2$ (RASSCF routine). The wave-functions obtained from these CASSCF calculations were posteriorly mixed by spin orbit coupling, where all 21 $S = 5/2$ states, 128 of the $S = 3/2$ states, and 130 of the $S = 1/2$ states were included (RASSI routine). The crystal field decomposition of the ground $J = 15/2$ multiplet of the $^6\text{H}_{15/2}$ term was executed with the SINGLE_ANISO module.

The energies of low-lying Kramer's doublets and the main components of the g tensor of the Dy(III) ions is shown in Table S9 and S10 for Fragment 1 and Fragment 2, respectively.



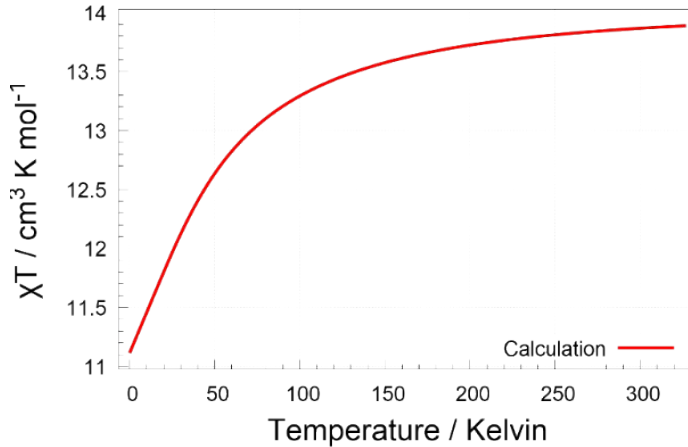


Fig. S18 *a)* Fragment 1 of Ni_5Dy_3 containing Dy1 employed for CASSCF calculations. All neighboring metals were replaced by diamagnetic ones, Ni→Zn and Dy→Lu. The violet arrow represents the anisotropy magnetic axes determined by the calculations for Dy1. Color code: Dy, cyan; Ni/Zn, green; Dy/Lu, light turquoise; C, grey; N, blue; O, red. *b)* Magnetization blocking barrier of fragment 1, where magnetic relaxation path, outlining the blocking barrier, is traced by the red lines, whose intensity scales the transition magnetic dipole matrix elements between the connected multiplet states. *c)* Calculated temperature dependence of χT .

Table S10. *ab initio* energy barrier and principal g-tensor for the Kramer doublets of Fragment 1 containing Dy1.

<i>ab initio</i> energy (cm ⁻¹)	<i>g</i> _x	<i>g</i> _y	<i>g</i> _z
0	0.032	0.070	18.853
111	0.558	0.935	14.766
199	1.861	2.505	11.899
294	8.016	6.469	4.161
386	1.396	2.953	10.697
420	0.142	4.031	13.240
480	0.677	1.899	16.899
562	0.036	0.106	19.440

The wavefunction for the ground state is 76% $|\pm 15/2\rangle$ + 15% $|\pm 11/2\rangle$, while the first excited state is 54% $|\pm 13/2\rangle$ + 36% $|\pm 9/2\rangle$.

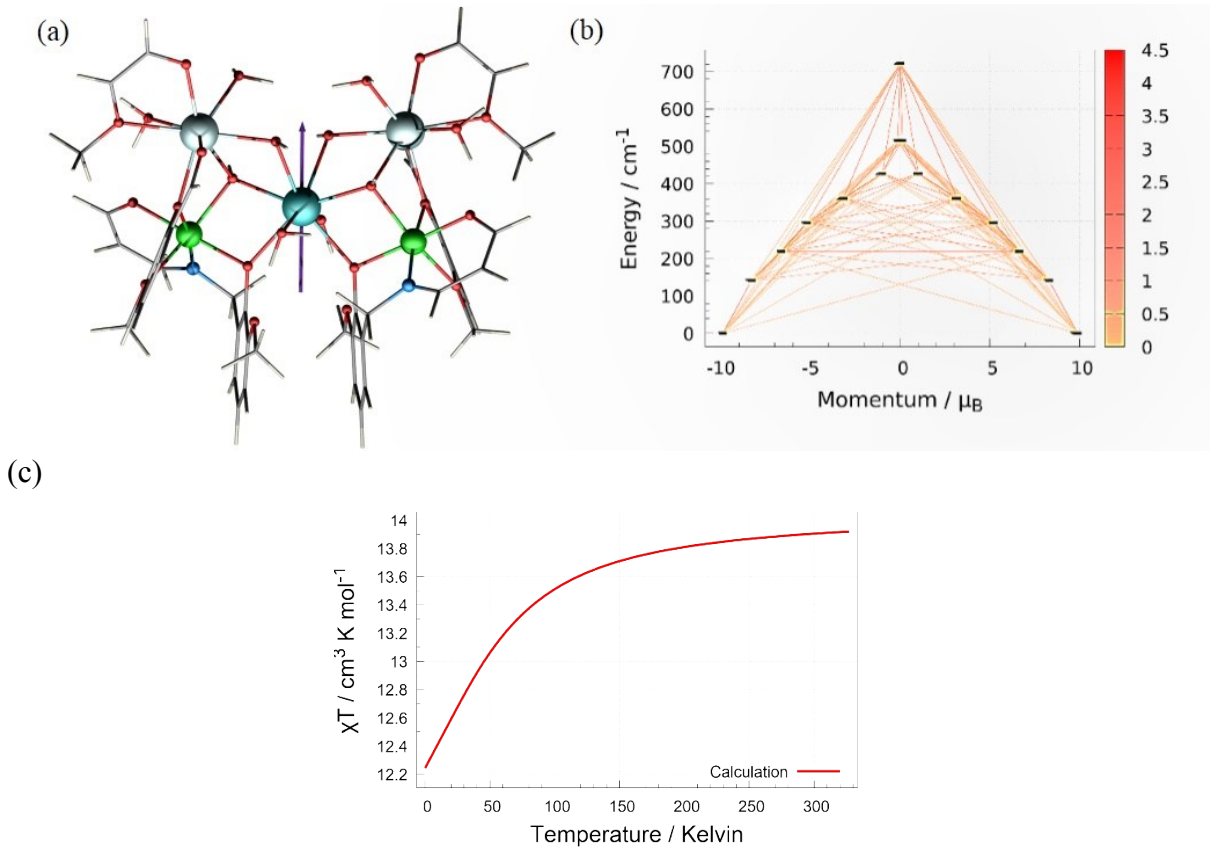


Fig. S19 *a)* Fragment 2 of Ni_5Dy_3 containing Dy2 employed for CASSCF calculations. All neighboring metals were replaced by diamagnetic ones, $\text{Ni}\rightarrow\text{Zn}$ and $\text{Dy}\rightarrow\text{Lu}$. The violet arrow represents the anisotropy magnetic axes determined by the calculations for Dy2. Color code: Dy, cyan; Ni/Zn, green; Dy/Lu, light turquoise; C, grey; N, blue; O, red. *b)* Magnetization blocking barrier of fragment 2, where magnetic relaxation path, outlining the blocking barrier, is traced by the red lines, whose intensity scales the transition magnetic dipole matrix elements between the connected multiplet states. *c)* Calculated temperature dependence of χT .

Table S11. *ab initio* energy barrier and principal g-tensor for the Kramer doublets of Fragment 2 containing Dy2.

<i>ab initio</i> energy (cm^{-1})	g_x	g_y	g_z
0	0.012	0.022	19.790
142	0.560	0.726	16.601
219	1.700	2.521	13.293
296	0.114	3.709	10.402
361	5.260	6.345	8.277
427	1.963	2.026	16.083
515	0.241	0.272	19.299
722	0.003	0.004	19.727

The wavefunction for the ground state is 98% $|\pm 15/2\rangle$, while the first excited state is 86% $|\pm 13/2\rangle + 6\% |\pm 13/2\rangle + 6\% |\pm 9/2\rangle$.

References

- S1.** R. A. Coxall, S. G. Harris, D. K. Henderson, S. Parsons, P. A. Tasker and R. E. P. Winpenny, *J. Chem. Soc. Dalton Trans.*, 2000, 2349–2356.
- S2.** M. Pinsky and D. Avnir, *Inorg. Chem.*, 1998, **37**, 5575–5582.
- S3.** S. Alvarez, D. Avnir, M. Llunell and M. Pinsky, *New J. Chem.*, 2002, **26**, 996–1009.
- S4.** D. Casanova, M. Llunell, P. Alemany and S. Alvarez, *Chem. Eur. J.*, 2005, **11**, 1479–1494.
- S5.** G. E. Kostakis, V. A. Blatov and D. M. Proserpio, *Dalton Trans.*, 2012, **41**, 4634–4640.
- S6.** G. E. Kostakis, I. J. Hewitt, A. M. Ako, V. Mereacre and A. K. Powell, *Phil. Trans. R. Soc. A*, 2010, **368**, 1509–1536.
- S7.** G. E. Kostakis and A. K. Powell, *Coord. Chem. Rev.*, 2009, **253**, 2686–2697.
- S8.** <http://www.sussex.ac.uk/lifesci/kostakislabs/picd/>; retrieved April 28, 2015.
- S9.** K. Wieghardt, K. Pohl, I. Jibril and G. Huttner, *Angew. Chem. Int. Ed. Engl.*, 1984, **23**, 77–28.
- S10.** A.-L. Barra, C. Paulsen, F. Bencini, A. Caneschi, D. Gatteschi, C. Paulsen, C. Sangregorio, R. Sessoli and L. Sorace, *ChemPhysChem*, 2001, **2**, 523–531.
- S11.** N. Berg, S. M. Taylor, A. Prescimone, E. K. Brechin and L. F. Jones, *CrystEngComm*, 2012, **14**, 2732–2738.
- S12.** R. T. W. Scott, L. F. Jones, I. S. Tidmarsh, B. Breeze, R. H. Laye, J. Wolowska, D. J. Stone, A. Collins, S. Parsons, W. Wernsdorfer, G. Aromi, E. J. L. McInnes and E. K. Brechin, *Chem. Eur. J.*, 2009, **15**, 12389–12398.